Comparison of Earthquake Damage Evaluation using Change Detection and Thematic Classification

Kyu-Seok Woo, Ellen Rathje, and Melba Crawford
University of Texas at Austin

Introduction

Because of the availability of high-resolution satellite imagery, remote sensing data has become an attractive source of data for identifying post-earthquake damage. Recently, several semi-automated methods for earthquake damage detection have been developed. These methodologies fall into two general categories: change detection and thematic classification. In change detection, both pre- and post-earthquake images are required, and pair-wise changes emerging from the pre-post comparison are attributed to earthquake damage. For thematic classification, only post-earthquake data are required, and earthquake damage is identified based on the distinguishing characteristics of features exhibited in the image. This study used pre– and post- earthquake satellite images from the 26 December 2003 earthquake in Bam, Iran ($M_w = 6.6$) as a test bed to demonstrate and compare the capabilities of these two methodologies to detect earthquake-related damage from satellite images.

Methodology

The change detection algorithm utilized in this study is based on the sample correlation coefficient computed for the co-registered pre-earthquake and post-earthquake image data. The change detection algorithm used in this study involves identification of changes in texture, based on the sample correlation coefficient for a windowed area:

$$r = \frac{n\sum PV_a PV_b - \left(\sum PV_a\right)\left(\sum PV_b\right)}{\sqrt{n\sum PV_a^{\,2} - \left(\sum PV_a\right)^2} \cdot \sqrt{n\sum PV_b^{\,2} - \left(\sum PV_b\right)^2}},$$

Where PV_a is the pixel value in the pre- earthquake image, PV_b is the corresponding pixel value in the post earthquake image, n is the number of pixels in the correlation window, and the summation is performed over all pixels in the window. For the correlation coefficient computation, a 15x15 pixel window was used to compute the sample correlation coefficient as significant changes caused by the earthquake were detected most effectively at this scale and computational requirements were reasonable [1].

The thematic classification approach uses only post-earthquake satellite images. For supervised analysis, which produces more accurate results, a subset of data associated with “damaged” and “undamaged” areas is identified for training the algorithm. One of the most commonly used supervised classification algorithms is the maximum likelihood method whereby the parameters of the probability density function for each class are estimated from the training data, and each unlabeled pixel is assigned to a relevant class based on the highest value of the likelihood function. Input data are typically assumed to have a Gaussian distribution, thereby requiring estimation of the sample mean and covariance matrix. Estimation of the covariance matrix is problematic if the dimension of the input space is high, but inadequate quantities of labeled training data are available. The problem was mitigated in this study by applying a Bayesian pair-wise feature selection algorithm in conjunction with a maximum likelihood classifier (BPC-FS, [2]). The BPC-FS algorithm identifies the feature or features that best distinguish each class pair based on the respective incremental contribution to classification accuracy. The method is also advantageous as it tunes the decision boundary between every pair of classes, thereby improving discrimination. Thirty-one features were considered in the BPC-FS analysis; the four spectral bands, eight texture measures (contrast: CON, dissimilarity: DIS, homogeneity: HOM, angular second moment: ASM, entropy: ENT, MEAN, variance: VAR, and correlation: COR) computed for three window sizes (6, 10, and 25 pixels), and edge density computed for the same three window sizes. Here, edge pixels were detected via a Canny filter[3], then the fraction of such pixels within a window computed.

Application to Bam, Iran Earthquake

High-resolution Quickbird images were acquired from the Bam, Iran, earthquake and used to assess urban damage patterns using thematic classification and change detection. For the thematic classification, only the post-earthquake satellite data were used. The ML classification analysis used only the most highly ranked features for each class pair, as chosen by the BPC-FS code. This resulted in using 14 of the original 31 features (blue, green, red, near infrared, MEAN6/3, ENT6/3, COR6/3, MEAN10/5, CON10/5, ENT10/5, ASM10/5, COR10/5, CON25/12, and COR25/12). For the change detection, both pre- and –post earthquake data were used. After co-registrating the images, the sample correlation coefficient (r) was computed for a 15 x 15 pixel window, and changed pixels were identified based on a specified threshold. For this study, the feature VAR31/15 and a threshold of 0.5 were used [1]. Because some image change is associated with vegetation and shadow due to variations in sun angle, seasons, etc., between image acquisitions, a mask that removes vegetation and shadow pixels from the changed pixels was applied. The identified damaged pixels from both methods were then used to compute damage intensity (DI), which is based on the percentage of pixels within a 100 x 100 pixel window (60 m x 60 m) that corresponds to earthquake damage. Only pixels that do not contain vegetation are considered in the DI calculation. The DI scale was defined as DI5 80-100% damage, DI4 (60-80% damage), and DI3 (40-60% damage). DI less than 40% was not considered significant based on visual examination of the damage in these areas.

The resulting damage intensities from the maximum likelihood (ML) classification and the change detection analysis are shown in Fig. 1, overlaid on the Quickbird images. The "moderately damaged" areas (DI3) are marked as green, the "severely damaged" areas (DI4) as blue, and the "fully destructed" areas (DI5) as red. Both methodologies indicate intense damage in the eastern part of the city (downtown), with significant areas labeled as DI4 and DI5. However, a detailed examination of the distribution of DI within the city reveals differences between the two analyses. The ML classification identifies a larger area of damage, with 38% of the image identified as DI3, DI4, or DI5, as opposed to 24% from change detection. In terms of the distribution of DI, the ML classification identified 5.16 km^2 of DI3, 2.63 km^2 of DI4, and 0.44 km^2 of DI5, while change detection identified 2.98 km^2 of DI3, 1.79 km^2 of DI4, and 0.48 km^2 of DI5. Thus, the biggest difference occurs between the identification of DI3 and DI4, which is apparent in Fig. 1 with significantly more D3 areas from the ML classification.

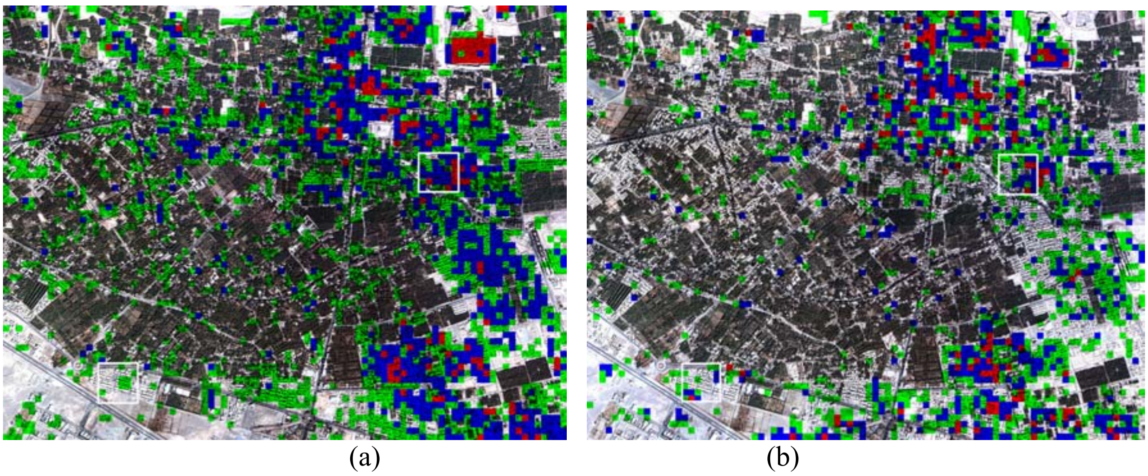

(a) (b)

Figure 1. Damage Intensity (DI) results from (a) Maximum-likelihood classification and (b) change detection analysis. Red represents DI5 (80-100% damage), blue represents DI4 (60-80% damage), and green represents DI3 (40-60% damage).

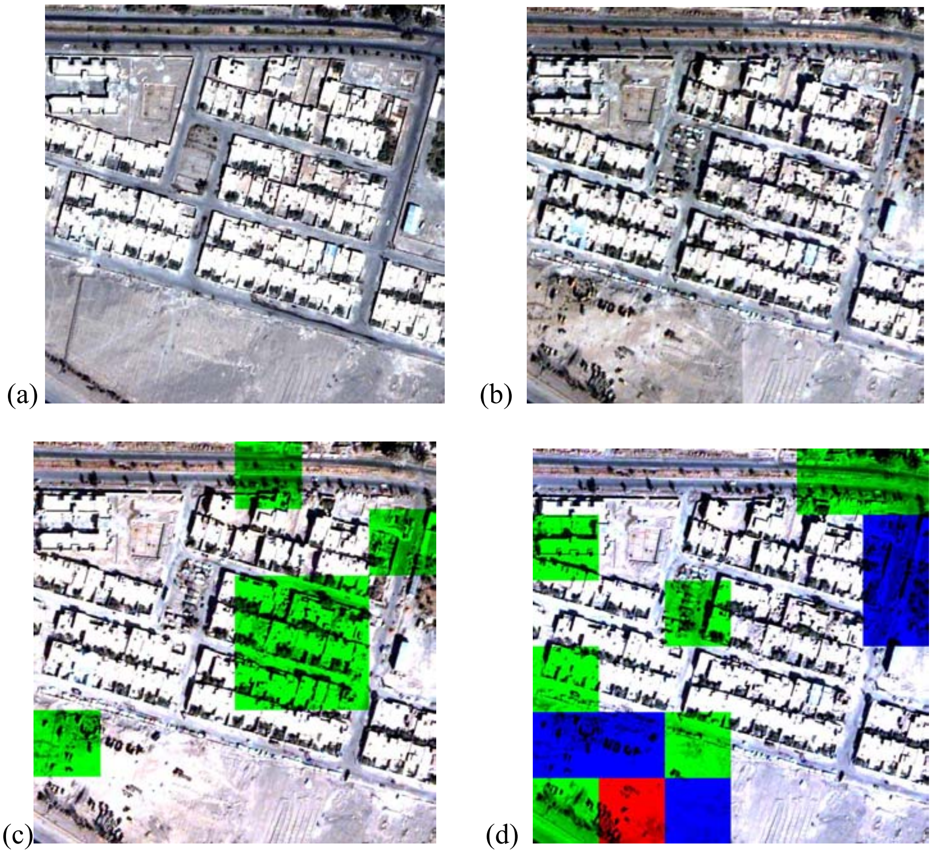

Figure 2. (a) Pre-earthquake and (b) post-earthquake image within southwestern Bam, and Damage Intensity results from (c) Maximum-likelihood classification and (d) change detection.

Fig. 2 shows pre- and post- earthquake images of a relatively non-damaged area within southwest Bam (Fig .1) and the damage intensity results from the two methodologies. The results from the ML classification (Fig. 2c) indicate some small areas of damage, although no damage can be visually identified in the image. The change detection results (Fig. 2d), however, reveal some areas of heavy damage (DI4 and DI5), mostly because of non-earthquake change. In particular, the eastern and southwestern parts of the area experienced change due to the presence of vehicles on roads and open ground. This result shows that, although the developed change detection algorithm removes non-earthquake changes associated with vegetation and shadow, the identification of other sources of non-earthquake change is one shortcoming of using change detection to evaluate earthquake damage patterns.

Fig. 3 shows an urban area in eastern Bam (Fig. 1) that was heavily damaged after the earthquake. In this area, the destruction is severe east of the north-south road, but less severe to the west of the road (Fig 3b). The maximum-likelihood classification (Fig. 3c) identifies DI4 damage throughout the image, with a concentration of DI5 along the eastern edge. Although the DI5 areas correspond with the heaviest damage within the image, some of the DI4 areas correspond with areas that are not severely damaged. This discrepancy is caused by confusion within the classification algorithm that incorrectly identifies some areas as damage. The results from change detection (Fig. 3d) identify DI4 and DI5 areas east of the road and mostly DI3 areas west of the road. This assessment of damage is in better agreement with the visual assessment of damage in the area, indicating that change detection can better distinguish between different intensities of severe damage.

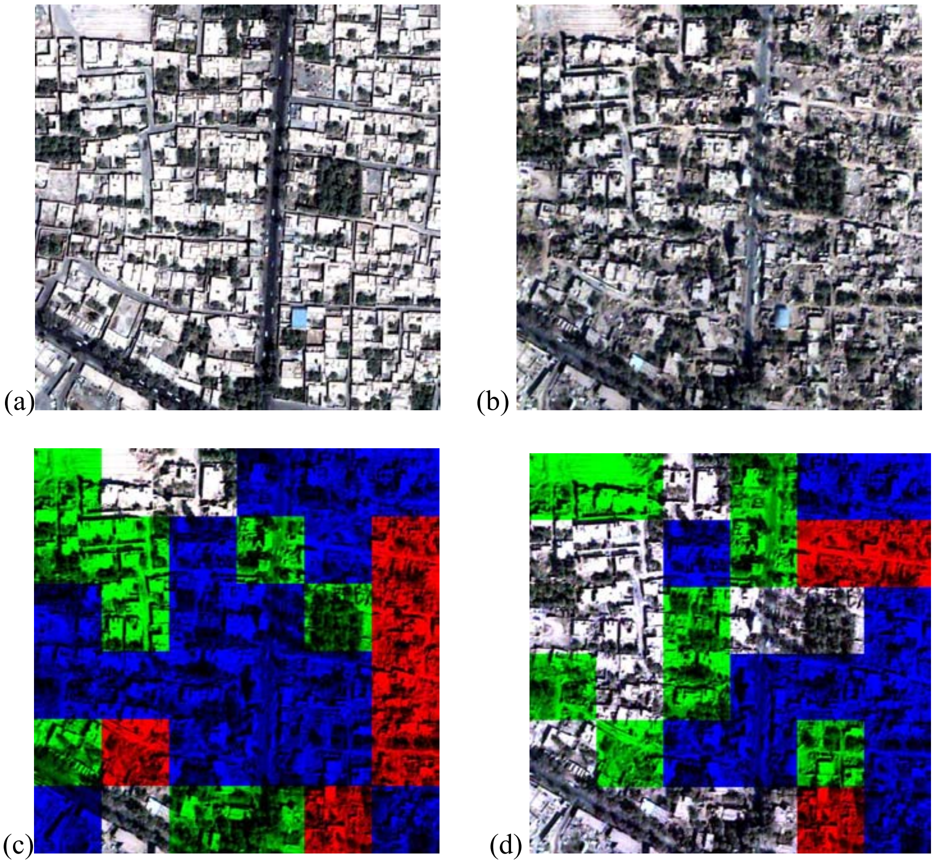

Figure 3. (a) Pre-earthquake and (b) post-earthquake image within eastern Bam, and Damage Intensity results from (c) Maximum-likelihood classification and (d) change detection

Conclusions

The purpose of this study was to compare earthquake damage evaluations from thematic classification and change detection using high-resolution satellite images. Based on this study of Bam, Iran, thematic classification generally identified more damage than change detection when considering the entire city. Additionally, thematic classification could not always distinguish between different levels of severe damage. Alternatively, change detection identified some significant non-earthquake change, particularly along roads, that resulted in an overestimation of damage in isolated areas. On-going research is focusing on developing a multi-resolution approach that integrates content dependent texture measures. The objective is to increase sensitivity while keeping the false detection rate low.

References

1. Rathje, E.M., Woo, K., Crawford, M., and Neuenschwander, A. "Earthquake Damage Identification using Multi-Resolution Optical Satellite Imagery," *International Geoscience and Remote Sensing Symposium*, IEEE, 2005, Seoul, South Korea,

2. Crawford, M.M., S. Kumar, M.R. Ricard, J.C. Gibeaut, and A. Neuenschwander. "Fusion of Airborne Polarimetric and Interfermetric SAR data for Classification of Coastal Environments." *IEEE Trans. Geoscience and Remote Sensing*, vol.37, 1306-1315, 1999

3. Canny, F. "A computational approach to edge detection ", *IEEE Trans. on Pattern. Anal. Machine Intell.*, 8(6):679-698,1986